Method of Calculating Frost Penetration Depth for Railway Subgrade Considering Thermal Characteristics of Multilayer Materials

Takaki MATSUMARU
Researcher,

Kenichi KOJIMA, Dr. Eng.
Senior Researcher,

Foundation & Geotechnical Engineering Laboratory, Structures Technology Division

Masao TOMINAGA
JR Kyushu Consultants Company Ltd. (Formerly a Guest Researcher at Railway Technical Research Institute)

Osamu MARUYAMA
Japan Railway Construction, Transport and Technology Agency

Makiko ISHIZUKA
Integrated Geotechnology Institute Ltd.

Method of Calculating Frost Penetration Depth for Railway Subgrade Considering Thermal Characteristics of Multilayer Materials

Takaki MATSUMARU
Researcher,

Kenichi KOJIMA, Dr. Eng.
Senior Researcher,

Foundation & Geotechnical Engineering Laboratory, Structures Technology Division

Masao TOMINAGA
JR Kyushu Consultants Company Ltd. (Formerly a Guest Researcher at Railway Technical Research Institute)

Osamu MARUYAMA
Japan Railway Construction, Transport and Technology Agency

Makiko ISHIZUKA
Integrated Geotechnology Institute Ltd.

In severely cold regions of Japan, a conventional countermeasure against frost heaving is to replace the silt and loam layers with a non-frost material. The depth for replacement is determined by the frost penetration depth obtained from one-dimensional analysis using only the freezing index based on the annual average air temperature. This means that the thermal characteristics of the materials comprising the railway track-bed are not taken into consideration. This paper examines the applicability of advanced Berggren's method as a new technique to determine the freezing penetration depth. This method makes it possible to take into account the thermal characteristics of multilayer materials. We also introduce experiments for the determination of thermal characteristics.

Keywords: *freezing penetration depth, advanced Berggren's method, multilayer materials*

1. Introduction

Countermeasures against frost heaving are important in the construction of railway track-bed in cold regions. Frost heaving occurs according to a complex set of conditions, including meteorological phenomena, air temperature, geography, geology, the heat characteristics of the track-bed and subgrade materials, and the groundwater level. In the current design standard for railway earth structures [1], the countermeasure against frost heaving involves replacing the clay and loam layer with a non-frost material (such as mechanically stabilized crushed stone) to a freezing penetration depth calculated by the following equation:

$$X = C\sqrt{F} \tag{1}$$

where X is the freezing penetration depth (cm) and F is the freezing index (℃·day). C is a constant number from 3 to 5, but in general has a value of 4.

This method has following problems:

(1) Parameter C in Equation (1) is constant number, so the freezing penetration depth is determined only from the freezing index without considering the heat characteristics and structural organization of the track-bed.

(2) Economical design is difficult, as it is not possible to take into account the effects of countermeasures such as replacing materials.

As an example, a frost heaving countermeasure evaluation is shown using Equation (1). Figure 1 illustrates the countermeasures executed experimentally by the Railway Technical Research Institute of the then JNR on the Chitose Line [2) 3)]. The experiment was conducted for four countermeasures, including insulation material and replacement, in the section between Eniwa Station and Osatsu Station from December 1979 to March 1980. From Equation (1), the frost penetration depth is calculated as 95.0 cm with the condition of C=4, using a freezing index of 563.4 (℃·day) as observed at Eniwa Weather Station, the nearest station to the experimental site. Here, the freezing penetration depth represents the distance between the ballast surface and a 0-degree line in the ground, so the frost penetration depth in the subgrade is 52.5 cm in (a), (b) and (c), and 10 cm in (d). In this experiment, frost heaving was observed only in the ballast-mat method (a). The results indicate that this calculation method may lead to excessive countermeasures because of difficulties in evaluating the thermal characteristics of materials. As shown in this example, appropriate calculation of the frost penetration depth may be difficult depending on the on-site soil conditions and countermeasure materials, making economical design of countermeasures impossible.

In this paper, we discuss the applicability of a calculation technique based on advanced Berggren's method to evaluate the frost penetration depth in order to overcome the problems outlined above. It is clear that this method enables calculation of the frost penetration depth in consideration of the thermal characteristics of track-bed materials and the effects of the countermeasure applied. In this method, evaluation of the thermal characteristics of track-bed materials

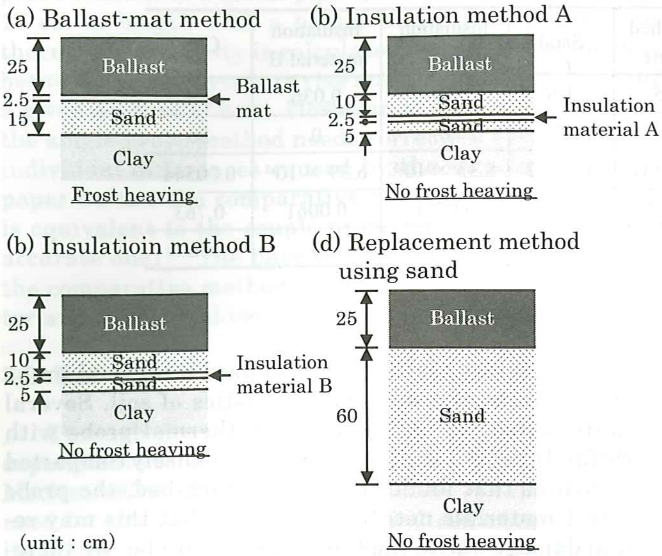

Fig. 1 Cross-sections of on-site countermeasure tests

is very important, but not many techniques enabling such measurement have been proposed. We therefore also propose a laboratory test method to determine the parameters required for design.

2. Application of advanced Berggren's method

Advanced Berggren's method[4)5)] is a one-dimensional calculation, but is capable of taking into account the thermal conduction of multilayer materials. In this chapter, we discuss the application of this method to evaluating frost heaving in railway track-bed.

2.1 Advanced Berggren's method

The frost penetration depth based on advanced Berggren's method is expressed by Equation (2). Though the framework of this equation is the same as that of Equation (1), parameter C is determined by the thermal characteristics of each material. This method is therefore a little more complex than Equation (1).

$$X = \lambda \sqrt{\frac{172800}{L/k}} \cdot \sqrt{F} \qquad (2)$$

where λ is a non-dimensional number related to cubic heat capacity, k is the thermal conductivity (cal/cm·s·℃) and L is the latent heat of fusion (cal/cm³). k and L represent the average values of each material weighted by layer thickness.

2.2 Method of calculating frost penetration depth

Figure 2 shows the flow of the frost penetration depth calculation using the advanced Berggren's method. This technique requires the meteorological conditions at the site, the cross-section shape and the thermal characteristics of the track-bed and subgrade materials.

In calculating the frost penetration depth, it is necessary to presume the value of X, and each parameter is then calculated. If the frost penetration depth X' obtained coincides with the assumed depth X, the calculation is complete. Otherwise, the calculation is repeated until X' agrees with X. The frost penetration depth is thus obtained from convergent calculation.

2.3 Example

To evaluate the suitability of this method for railway track-bed, we applied the calculation technique based on advanced Berggren's method to the countermeasure experiments described above. Table 1 shows the thermal characteristics of the track-bed, subgrade and countermeasure materials[3)]. Based on the data observed at the nearest weather station, the freezing index, freezing period and annual average temperature are set at 563.4 (℃·day), 114 (days), 6.7 (℃).

Table 2 shows the calculation results, namely the frost penetration depth from the surface of the track-bed, and Fig. 3 shows the frost penetration depth of the subgrade. In addition to the results obtained from advanced Berggren's method, the results from Equation (1) in the conditions with C=4 are also shown in Table 2 and Fig. 3. Though the experimental results were reported qualitatively rather than quantitatively, the results of calculation based on the advanced Berggren's method coincide with the tendency of countermeasure effects different from those obtained by Equation (1). This demonstrates the

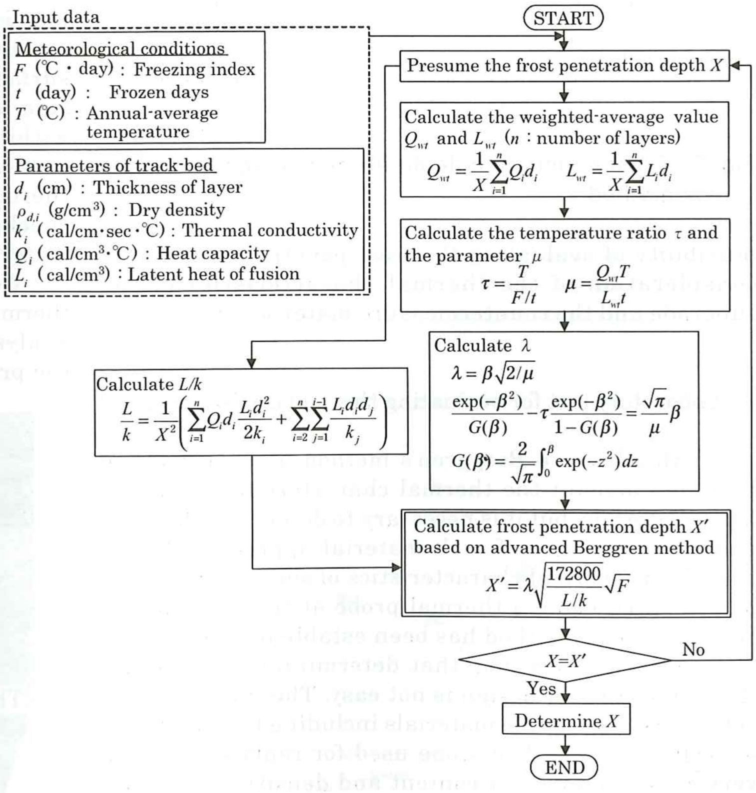

Fig. 2 Flow of frost penetration depth calculation method for railway track-bed based on advanced Berggren's method

Table 1 Thermal characteristics

Parameter	Symbol	Unit	Crushed stone	Sand	Insulation material A	Insulation material B	Clay
Dry density	ρ_d	g/cm^3	1.5	1.6	0.040	0.036	1.4
Water content	w	%	2	15	0	0	50
Thermal conductivity	k	cal/cm・sec・℃	0.00131	0.00492	8.33×10^{-5}	6.39×10^{-5}	0.00544
Heat capacity	Q	cal/cm^3・℃	0.278	0.452	0.0051	0.0061	0.763
Latent heat of fusion	L	cal/cm^3	2.4	19.2	0	0	56

Table 2 Calculation results (frost penetration depth from the surface of the track-bed)

Countermeasure method	Advanced Berggren's method (cm)	Conventional method (cm)
Ballast-mat method	60	95
Insulation method A	49	95
Insulation method B	48	95
Replacement method using sand	83	95

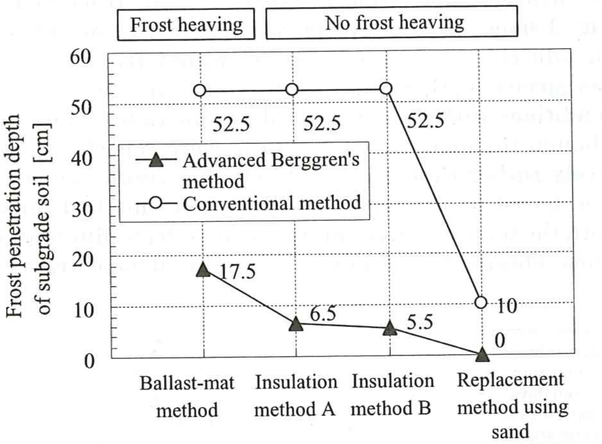

Fig. 3 Frost penetration depth for each countermeasure method

possibility of evaluating the frost penetration depth in consideration of the thermal characteristics of the subgrade and the countermeasure material used.

3. Laboratory test for evaluating thermal conductivity[6)-8)]

With advanced Berggren's method, it is possible to take into account the thermal characteristics of multi-layer materials, but it is necessary to determine the thermal characteristics of each material appropriately. Although the thermal characteristics of soil materials can be measured using a thermal probe at the site, no specific measuring method has been established for laboratory tests, which means that determining the thermal characteristics for design is not easy. The thermal characteristics of subgrade materials including loam and clay, as well as the crushed stone used for replacement, are very sensitive to water content and density, so it is important to determine the characteristics with due consideration of on-site conditions.

3.1 Test method

In laboratory testing, we also used a thermal probe to measure the thermal characteristics of soil. Several metallic wires are installed in the thermal probe with paraffin. In order to apply the probe to densely compacted soil such as that found in railway track-bed, the probe and test materials need to be tamped, but this may result in damage due to the fineness of the probe. We therefore attempted to strengthen the probe by using thick metallic wire, but this method does not satisfy the assumption of the analysis that the probe has a zero diameter. In this paper, we attempt to measure the thermal conductivity of crushed stone and subgrade materials by sandwiching a probe and a thermo couple between two specimens as shown in Fig. 4[6)]. The merit of this method is that it does not add any load due to the compacting of the test specimen to the probe and thermo couple. A pair of molds is used for the specimen, 160 mm in length and width, and 80 mm in depth, based on a value of 160 mm, or 4 times 40 mm, which is the maximum diameter of the crushed stone. The procedure for making the specimen is as follows: First, a spacer for sensing elements is made on the undersurface of each mold, and the upper surface is capped after compaction. Then, the cap on the side of the spacer is removed, and the sensors are set within the two molds. In the probe method, the contact conditions of the sensors and soil are important because thermal diffusion occurs in all directions. We therefore checked the contact conditions of the probe and test material by inserting pressure-sensitive film.

We used the single-probe method for measurement of thermal conductivity and the comparative method for data analysis. In the single-probe method, it is assumed that the probe is zero in diameter and infinite in length. The

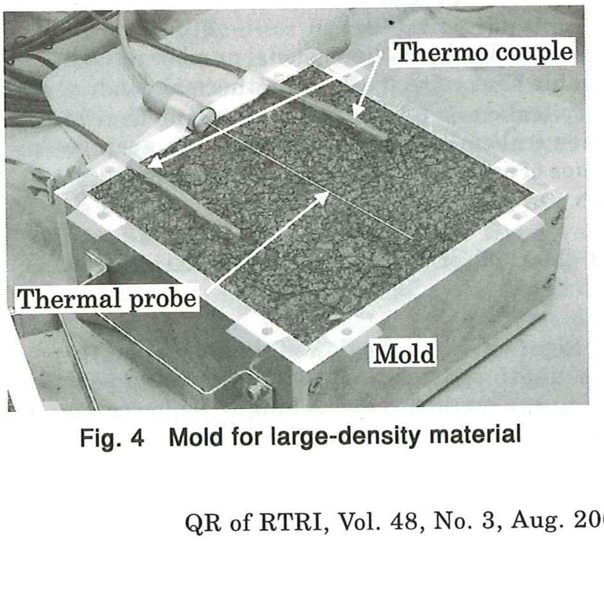

Fig. 4 Mold for large-density material

probe consists of a metal pipe of 1.3 mm in diameter and 15 cm in length with a heater and a heat gauge. The thermal conductivity is calculated from the relationship between the temperature rise and the heating time, and a given amount of heat. However, the value obtained by the single-probe method needs correction because of the individual differences caused by the structure. In this paper we use the comparative method, whose accuracy is equivalent to the couple probe method (i.e. the most accurate one)[9]. The base thermal conductivity used in the comparative method is 0.00134cal/cm/sec/℃ for water and 0.00526cal/cm/sec/℃ for ice[10].

3.2 Test case

Through the proposed laboratory test, we conducted experiments targeting the site of a new Shinkansen line. Mechanically stabilized crushed stone is expected to be used for the railway track-bed, and the adopted size of its pieces is less than 31.5 mm according to the specimen size. From compaction testing (using the E-b method) and density testing of soil particles, the maximum dry density $\rho_{d\max}$ is 2.09 g/cm^3, w_{opt} is 6.2 %, and the particle density G_s is 2.72. The thermal conductivity depends on the density, water content and temperature, so the experimental conditions were determined as shown in Table 3. Five specimens were measured with different water content and density in an unfrozen state (20 ℃) and in a frozen state (-10℃) (only specimen No.5 was measured in an unfrozen state).For the loam and clay, we used materials obtained from a site in the Shichinohe area of Aomori Prefecture. The specimens were made from disturbed materials to satisfy the conditions of on-site dry density and water content. The dry density and water content is 1.09 g/cm^3 and 52% for the loam and 0.82 g/cm^3 and 82% for the clay, as measured from a 100-cc sample of the materials. Table 4 shows the test case. Taking into consideration the materials used, two specimens are tested under the same conditions.

Table 3 Test case (crushed stone)

Case	D (%)	w (%)	Temperature conditions
1	95	6.2	20℃, -10℃
2	95	6.2	20℃, -10℃
3	95	4.7	20℃, -10℃
4	90	6.2	20℃, -10℃
5	90	6.2	20℃

Table 4 Test case (loam and clay)

Case	Material	Temperature conditions
6	Loam	20℃, -10℃
7	Loam	20℃, -10℃
8	Clay	20℃, -10℃
9	Clay	20℃, -10℃

3.3 Test results

Each measurement was taken three times at 20℃ and -10℃. Figure 5 shows an example of the temperature

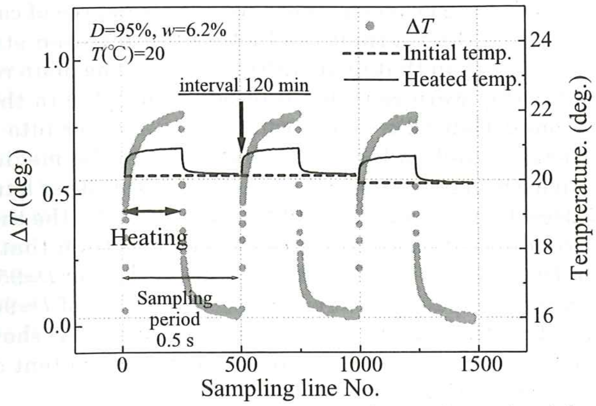

Fig. 5 Example of measuring thermal conductivity

increase during measurement of the thermal conductivity and the decrease after heating was stopped. The horizontal axis represents the number of days of sampling, the right vertical axis shows the temperature and the left vertical axis gives the temperature difference ΔT. ΔT (●), with values measured every 0.5 s, shows three waves representing three measurements. In order to allow the temperature of the specimen to return to normal, an interval of about 120 minutes was left between stopping heating and the next measurement in all cases.

Figure 6 shows the measurement results (−, −) and the averages (●: 20℃, ▲: -10℃) in each case. In Cases

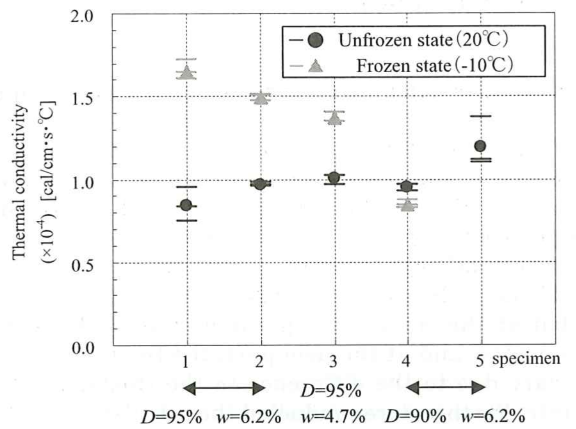

(a) Thermal conductivity of crushed stone

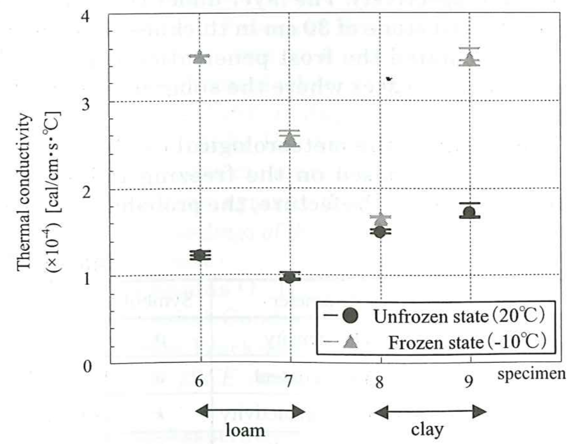

(b) Thermal conductivity of loam and clay

Fig. 6 Measurement results of thermal conductivity

1, 2 and 3 using crushed stone with a 95% degree of compaction (D), the thermal conductivity in a frozen state was greater than that in an unfrozen state. The main reasons for this were considered to be an increase in thermal conductivity due to the conversion of water into ice by freezing, and an increased continuity in the medium due to ice bridges in the soil particles. On the other hand, in Cases 4 and 5 using crushed stone of D=90%, the thermal conductivity in a frozen state was less than that in an unfrozen state, which is the opposite of that for D=95%. From the compaction characteristics, a value of D=90% means that the samples are not well compacted. As shown by the results of Cases 1, 2 and 3, the water content did not affect the thermal conductivity.

For loam and clay, the thermal conductivity was steady in an unfrozen state, but varied in a frozen state. In this paper, we conduct experiments on frozen specimens at -10 ℃ to avoid the transition region from +5 to -5℃. However, the temperature in the experiment was not steady, so the void water might be in a different state in each case.

In this experiment, the thermal conductivity of the loam and clay did not vary, and was steady except when in a frozen state. Using this conductivity, two-dimensional finite element analysis was conducted to examine the temperature behavior on the experimental track-bed in the Shichinohe area [11]. The results obtained from this simulation show a close correlation with the experimental results, demonstrating that this thermal conductivity can be considered appropriate [12].

4. Example of calculating the frost penetration depth

We conducted frost penetration depth calculation aimed at the slab track on the earth structure of a new Shinkansen line, and compared the results with those obtained from Equation (1). Figure 7 shows a cross-section of the railway track structure used in this calculation. Usually, the concrete thickness of a slab track is 30 cm, but at the center of separated slab track used for storing snow and at the pole part, the frost penetration may vary due to the difference in the thickness of the concrete. We therefore conducted the calculation on three cross-sections with a concrete thickness of 10 cm, 30 cm and 70 cm respectively. The layer under the concrete consists of crushed stone of 30 cm in thickness and subgrade soil. We calculated the frost penetration depth of three cross-sections in cases where the subgrade soil is clay or loam.

Table 5 shows the meteorological conditions used in this calculation. Based on the freezing index at three locations in Aomori Prefecture, the probabilistic freezing index was analyzed with a return period of 100 years. The three locations used were Hachinohe, Misawa and Towada, with the freezing index increasing and the annual average temperature decreasing according to this sequence. The thermal conductivity is based on the experimental results described in Chapter 3. Table 6 shows the input parameters determined. The thermal conductivity should be changed depending on the state (i.e. frozen or unfrozen) because it differs between the two states. However, changing the conductivity according to the state is not realistic since the calculation becomes more complex due to the increase of convergent calculation. The thermal conductivity of the crushed stone is determined as the average of the values in the frozen and unfrozen states for D=95% (in cases 1 and 2) taking into consideration the probability of freezing, and the conductivity of the subgrade soil was taken as the value in the unfrozen state. It is difficult to measure the heat capacity Q and latent heat of fusion L, so these values were determined from Equations (3) and (4) [13].

$$Q = (0.17 + 0.0075w) \cdot \rho_d \quad (3)$$

$$L = 0.8w\rho_d \quad (4)$$

where w represents the water content (%) and ρ_d is the dry density (g/cm^3).

Table 7 shows the calculation results. This table shows the results in the case where the subgrade soil was loam or clay for each meteorological condition, and the results

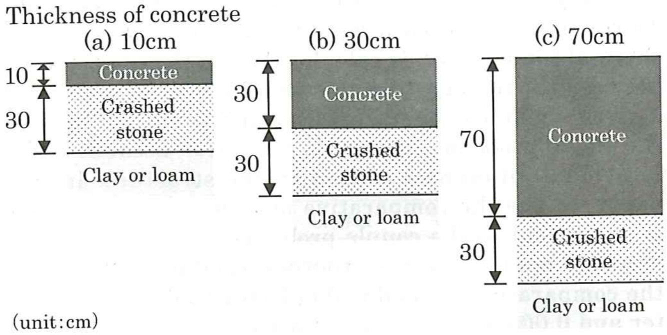

Fig. 7 Cross-sections of the track structure used in this calculation

Table 5 Meteorological conditions

Area	Freezing index (℃ · day)	Frozen days (days)	Annual average temperature (℃)
Hachinohe	324.4	110	10
Misawa	360.7	114	9.9
Towada	495.0	125	9.4

Table 6 Thermal characteristics

Parameter	Symbol	Unit	Concrete	Crushed stone	Loam	Clay
Dry density	ρ_d	g/cm³	2.35	1.98	1.09	0.82
Water content	w	%	—	6.2	52.0	82.0
Thermal conductivity	k	cal/cm · sec · ℃	0.00611	0.00123	0.00109	0.00160
Heat capacity	Q	cal/cm³ · ℃	0.6	0.430	0.605	0.644
Latent heat of fusion	L	cal/cm³	0	9.82	45.34	53.79

Table 7 Results of frost penetration depth

Area	Subgrade soil	Advanced Berggren's method			$C\sqrt{F}$
		(a) 10 cm	(b) 30 cm	(c) 70 cm	(C=4)
Hachinohe	Loam	44.0	60.3	80.2	72.0
	Clay	43.6	60.3		
Misawa	Loam	45.4	61.4	84.0	76.0
	Clay	44.8	61.2		
Towada	Loam	50.6	66.0	97.7	89.0
	Clay	49.8	65.4		

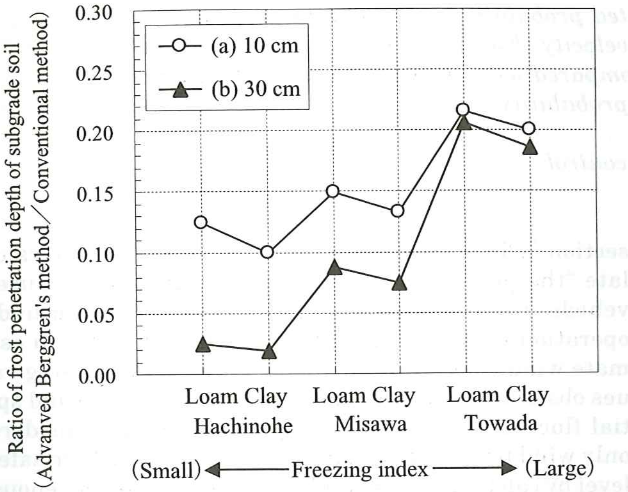

Fig. 8 Ratio of frost penetration depth of subgrade soil

obtained from Equation (1) were also shown in the condition of C=4. In the results of calculation adopting the advanced Berggren's method, the frost penetration depth could be calculated with due consideration not only of the meteorological conditions but also of the subgrade soil. Here, the frost penetration depth was the depth distance between the surface of the concrete and the 0-degree line in the ground. This means that the subgrade soil would be frozen at a frost penetration depth of 40 cm for (a), 60 cm for (b) and 100 cm for (c). In case (c), it is shown that the subgrade soil was not frozen, so the frost penetration depth was the same for both kinds of subgrade soil. Furthermore, the frost penetration depth of only the subgrade soil was calculated from the results as shown in Table 7, and the ratio of the depth obtained from the advanced method to the depth from the conventional method was as shown in Fig. 8. The results of case (c) (with a concrete thickness of 70 cm) were not considered in this figure. The figure indicates that the frost penetration depth was much less than with the conventional method, depending on the meteorological conditions and the cross-section of the track structures. The advanced Berggren's method would therefore enable provision of a more economical countermeasure method against frost heaving.

5. Conclusions

In calculating the frost penetration depth necessary for working out a countermeasure against frost heaving, we studied an advanced Berggren's method and evaluated its merits, such as enabling quantitive consideration of the thermal characteristics of the soil and the effects of the countermeasure method. Furthermore, we proposed laboratory testing to measure the thermal characteristics of soil, and showed the values to be used as parameters for design. From the trial calculation, it was found that the proposed method would enable provision of a more economical countermeasure method. In the future, we plan to evaluate countermeasure methods other than replacement, such as insulation techniques and cement soil stabilization.

References

1) Railway Technical Research Institute, Design standards for railway structures and commentary (earth structures), 1992 (in Japanese).
2) Ooi S., Countermeasure method for railway track-bed, *Tsuchi-to-kiso*, pp.47-52, 1981 (in Japanese).
3) Sunaga M., Noguchi T., Ooi S., Measurement of countermeasures against frost heaving on the Chitose Line, *Railway Techinical Research Institute Report*, 1983 (in Japanese).
4) Jumikis, Alfred R., Thermal Geotechnics, *Rutgers Uni. Press*, pp.185-224, 1977.
5) Aldrich, Harl. P., Frost Penetration below Highways and Airfields, *H.R.B. Bulletin*, No.135, pp.124-149, 1976.
6) Ishizuka M., Maruyama O., Aoki H., Kojima K., Tominaga M. and Ishiyama T., Thermal Conductivity Measurement of high bulk density soil using the single thermal probe method, *Proceedings of the 40th Japan National Conference of Geotechnical Engineering*, 2005 (in Japanese).
7) Ishizuka M., Kojima K, Tominaga M., Maruyama O., Aoki H. and Ishiyama T., Measurement of the thermal conductivity of crushed stone, *Proceedings of the 60th JSCE Annual Meeting*, 2005 (in Japanese).
8) Kojima K., Maruyama O., Aoki H., Noda G. and Ishizuka M., Measurement of the thermal conductivity of loam and clay by laboratory testing, *Proceedings of the 60th JSCE Annual Meeting*, 2005 (in Japanese).
9) Kasubuchi T., Research into the thermal conduction of soil, *Agriculture Technical Research Institute Report*, B, No.33, pp.1-54, 1982 (in Japanese).
10) National Astronomical Observatory of Japan, Scientific Chronology, 2002 (in Japanese).
11) Maruyama O., Aoki H., Noda G., Tamura Y. and Kojima K., On-site measurement of temperature for countermeasures against frost heaving of railway track-bed, *Proceedings of the 60th JSCE Annual Meeting*, 2005 (in Japanese).
12) Aoki H., Maruyama O., Kojima K., Matsumaru T. and Hori K., Thermal Conduction Analysis of Temperature in Railway Track-bed for Frost Heaving, *Proceedings of the 61st JSCE Annual Meeting*, 2006 (in Japanese).
13) Japan Road Association, Design standard for the drainage of road earth structures, pp.244-250, 1987 (in Japanese).